Journal of Colloid and Interface Science 338 (2009) 48–55

Contents lists available at ScienceDirect

Journal of Colloid and Interface Science

www.elsevier.com/locate/jcis

Selenium adsorption to aluminum-based water treatment residuals

James A. Ippolito [a,*], Kirk G. Scheckel [b], Ken A. Barbarick [c]

[a] USDA-ARS-Northwest Irrigation and Soils Research Laboratory, 3793 North 3600 East, Kimberly, ID 83341, United States
[b] National Risk Management Research Laboratory, U.S. Environmental Protection Agency, 5995 Center Hill Ave., Cincinnati, OH 45224, United States
[c] Department of Soil and Crop Sciences, Colorado State University, Fort Collins, CO 80523, United States

ARTICLE INFO

Article history:
Received 29 April 2009
Accepted 10 June 2009
Available online 14 June 2009

Keywords:
Inner-sphere complexation
Outer-sphere complexation
Selenate
Selenite
X-ray absorption spectroscopy

ABSTRACT

Aluminum-based water treatment residuals (WTR) can adsorb water- and soil-borne P, As(V), As(III), and perchlorate, and may be able to adsorb excess environmental selenium. WTR, clay minerals, and amorphous aluminum hydroxide were shaken for 24 h in selenate or selenite solutions at pH values of 5–9, and then analyzed for selenium content. Selenate and selenite adsorption edges were unaffected across the pH range studied. Selenate adsorbed on to WTR, reference mineral phases, and amorphous aluminum hydroxide occurred as outer sphere complexes (relatively loosely bound), while selenite adsorption was identified as inner-sphere complexation (relatively tightly bound). Selenite sorption to WTR in an anoxic environment reduced Se(IV) to Se(0), and oxidation of Se(0) or Se(IV) appeared irreversible once sorbed to WTR. Al-based WTR could play a favorable role in sequestering excess Se in affected water sources.

Published by Elsevier Inc.

1. Introduction

Selenium is a semi-metallic, naturally occurring trace element commonly found in strata and soils derived from certain types of marine sediments. These sediments tend to dominate in the western USA, and thus environmental issues associated with Se are numerous in this region (e.g., Kesterson Reservoir, CA; Kendrick Reclamation Project Area, Wyoming; Colorado River near Grand Junction, CO). Selenium risks at these sites include bioaccumulation, reproduction failure, deformities, and die-off of migratory waterfowl, fish, insects, and plants [1–3]. In these natural systems Se can occur in four different oxidation states (Se^{2-}, Se^{0}, Se^{4+}, Se^{6+}); selenate (Se^{6+}; Se(VI)) and selenite (Se^{4+}; Se(IV)) are commonly found in arid regions with form dependent on redox conditions. Selenate can occur in oxidized soils and alkaline surface waters, and is mobile due to its high water solubility and poor soil adsorption characteristics. Selenate can be reduced to selenite, with selenite more readily accumulated by aquatic organisms. Because of the tendency of Se to accumulate in soil and water ecosystems, treatment strategies which target the removal of readily available, water-borne selenium should help reduce the bioaccumulation potential. As a remediation strategy, WTR may be a useful sorbent for Se in these ecosystems but information is sparse.

Alum [$Al_2(SO_4)_3{\cdot}14H_2O$] is commonly used in the drinking water treatment process for particulate flocculation and water clarification. Water treatment residuals (WTRs), a waste product of drinking water treatment facilities, tend to have a mineral form similar to amorphous $Al(OH)_3$ when alum is utilized. Because of their amorphous nature, WTRs have a large surface area (up to 105 $m^2\ g^{-1}$) [4] and are highly reactive. They have the proven ability to adsorb tremendous quantities of P [5,6] and have been shown to adsorb other oxyanions such as As(V), As(III), and ClO_4^- [7,8]. Water treatment residuals may also adsorb selenium species although this phenomenon and the bonding mechanisms have yet to be documented.

Adsorption of trace element oxyanions, such as selenate and selenite, on to surface functional groups of metal oxide mineral phases (such as WTR) is a major mechanism of removal from aqueous solution [9]. However, the adsorption process is not simply a competitive ion-exchange reaction because differences in adsorption and desorption isotherms typically show significant hysteresis [10]. Balistrieri and Chao [11] noted that selenite adsorbed much more strongly than selenate to goethite (FeOOH). This phenomenon was explained by Hayes et al. [12] who used extended X-ray absorption fine structure (EXAFS) analysis to study Se adsorption on to goethite (FeOOH). The authors showed that selenate formed a weakly bonded outer-sphere complex while selenite formed a strongly bonded inner-sphere complex. Peak and Sparks [13] used EXAFS to denote selenate adsorption on hematite (purely inner-sphere complexation), goethite and hydrous ferric oxide (a mixture

Abbreviations: EXAFS, extended X-ray absorption fine structure; ICP-AES, inductively coupled plasma-atomic emission spectroscopy; WTR, aluminum-based water treatment residuals; XAS, X-ray absorption spectroscopy; XAFS, X-ray absorption fine structure; XRD, X-ray diffraction analysis.

* Corresponding author. Fax: +1 208 423 6555.
E-mail address: jim.ippolito@ars.usda.gov (J.A. Ippolito).

0021-9797/$ - see front matter Published by Elsevier Inc.
doi:10.1016/j.jcis.2009.06.023

of outer- and inner-sphere complexes). Manceau and Charlet [14] identified similar selenate binding chemistry on goethite. Peak [15] further studied selenate and selenite adsorption on to hydrous aluminum oxide, noting that selenate formed outer-sphere while selenite formed a mixture of outer- and inner-sphere complexes. Wijnja and Schulthess [16] also noted that selenate formed mainly outer-sphere associations on aluminum oxide.

Aluminum-based WTR consists of a mixture of amorphous $Al(OH)_3$ and other constituents reflective of area geology, such as clay minerals, oxides, and calcite. Each solid phase will interact differently with Se, hence different quantities of Se may be removed. For instance, Goldberg and Glaubig [17] observed that selenite adsorption onto kaolinite was approximately twice that of montmorillonite, likely due to greater kaolinitic edge surface area. Both minerals showed maximum adsorption at pH 5, with adsorption decreasing with increasing pH. This confirmed similar results for kaolinite and montmorillonite found by Bar-Yosef and Meek [18]. Goldberg and Glaubig [17] also found that selenite adsorption on calcite increased from pH 6–8, was at a maximum between 8 and 9, and decreased at greater pH values. The authors noted that the adsorption maximum of calcite was four to eight times greater than the clay mineral phases. Our objectives were to determine if Al-based WTR could sequester Se(VI) and Se(IV), and to identify Se adsorption chemistries onto the mineral phases present in WTR.

2. Materials and methods

2.1. Materials

Water treatment residuals were obtained from the Fort Collins, Colorado, USA drinking water treatment facility. Fort Collins utilizes alum to flocculate suspended colloids during water clarification. The WTR were air-dried and then passed through a 2-mm sieve prior to analysis. The WTR total elemental composition, except for Se and Si, was determined by a modified $HClO_4$-HNO_3-HF-HCl digestion [19] with the digestate analyzed using inductively coupled plasma-atomic emission spectroscopy (ICP-AES) (Table 1). Total Se and Si content were determined using SW-846 Method 3050B [20] and aqua regia-HF [21] in a closed vessel, respectively, followed by ICP-AES analysis. Total N was determined by a H_2SO_4 digestion [22]. The NO_3-N and NH_4-N were determined using a 2 M KCl extract [23], pH and electrical conductivity (EC) using a saturated paste extract [24,25], organic matter content using the Walkley–Black procedure [26], and CEC via the Rhoades method [27].

Table 1
Total chemical characteristics of Fort Collins, CO, water treatment residuals (WTR).

Property	WTR
Si (%)	19.7
Al (g kg^{-1})	74.7
Fe (g kg^{-1})	17.8
Ca (g kg^{-1})	15.7
Mg (g kg^{-1})	4.5
Mn (g kg^{-1})	0.8
Se (mg kg^{-1})	<0.1
Cu (mg kg^{-1})	47.6
Zn (mg kg^{-1})	53.3
Ni (mg kg^{-1})	10.9
Mo (mg kg^{-1})	<0.1
Cd (mg kg^{-1})	<0.1
Cr (mg kg^{-1})	19.1
Sr (mg kg^{-1})	31.1
B (mg kg^{-1})	91.6
Ba (mg kg^{-1})	95.2
Pb (mg kg^{-1})	<2.5
Total N (%)	0.4
NH_4–N (mg kg^{-1})	70.1
NO_3–N (mg kg^{-1})	44.0
pH	6.9
EC (dS m^{-1})	0.7
O.M. (%)	6.3
CEC ($cmol_c$ kg^{-1})	39.3

The WTR were also examined using X-ray diffraction analysis (XRD; SCINTAG Model XDS 2000 XGEN-4000, Thermo ARL, Switzerland). This analysis required the sample to be ground using a porcelain mortar and pestle, then packed into a 2.54-cm diameter by 0.32-cm deep holder as a packed dry powder mount. The sample was analyzed from 5° to 55° 2θ in an XRD containing a copper target. Box car smoothing was used and K-α2 stripping was performed using K-α1 and K-α2 as 1.540562 and 1.544390, respectively.

The XRD analysis verified that the WTR contained quartz, feldspar, calcite, illite/smectite, and kaolinite (Fig. 1). As a note, other researchers have shown various degrees of Se sorption to kaolinite, smectite, calcite, and amorphous Al (hydr)oxides [17,28,29]. Therefore, to support or reject the presence of these mineral phases as Se adsorbents, reference mineral phases were selected to resemble Se sorption dynamics of the dominant WTR mineral phases. We believe the surface properties of these pure phase minerals should resemble or mimic Se sorption by the mineral assemblages present in Fort Collins, Colorado, USA WTR. A low defect kaolinite, Ca-rich montmorillonite, and an illite–smectite mixed layer clay were purchased from the Clay Minerals Society Source Clays Repository (West Lafayette, IN), while calcite was purchased from American Educational Products (Fort Collins, CO) and pulverized prior to use. Amorphous Al (hydr)oxide was created following the method outlined by Kabengi et al. [30], where $AlCl_3$ was dissolved in 100 mL of distilled-deionized water, titrated drop-wise with NaOH to pH 6.5, allowed to stand overnight, centrifuged, solution discarded, and solid dried overnight at 65 °C. The dried solid was pulverized prior to the Se adsorption experiment.

2.2. Experiment 1 approach

In 100 mL of 0.05 M NaCl solution, 2.5 g WTR, clay mineral standard, or amorphous Al (hydr)oxide was mixed with either 14.4 mg Na_2SeO_4 (Se(VI)) or 13.1 mg Na_2SeO_3 (Se(IV)) to provide a Se concentration of 60 mg L^{-1}. Solution pH was varied from 5 to 9 and samples were shaken for 24 h at 120 rpm on a reciprocating shaker. Triplicate WTR mixtures were utilized, but only single reference clay minerals and amorphous $Al(OH)_3$ samples were used due to limited quantities available. The Se(VI) experiment was exposed to laboratory atmospheric conditions while the Se(IV) samples were exposed to a stream of N_2 gas at ~28 kPa to avoid oxygen

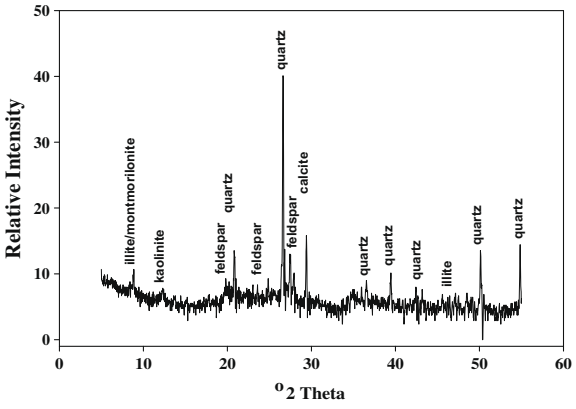

Fig. 1. X-ray diffraction analysis of Fort Collins, CO, USA aluminum-based water treatment residuals (WTR).

exposure. Following shaking, the Se(VI) mixtures were then centrifuged, the liquid decanted, and the solids were dried under atmospheric conditions at 25 °C; the Se(IV) samples were centrifuged, decanted, and then dried at 25 °C under reduced conditions in an anaerobic glove bag with a gas phase consisting of 90% N_2 and 10% H_2. The supernatant was analyzed for either Se(VI) or Se(IV) via hydride generation using ICP-AES. Adsorbed WTR Se concentrations were statistically analyzed at an $\alpha = 0.05$ using a completely randomized design in the Proc GLM model, SAS software version 9.1 [31]. In addition, the Se(IV) data were log transformed prior to analysis to meet conditions of normal distribution; however, Se(IV) data are presented as untransformed.

Dried, solid phase Se(VI) or Se(IV) samples were placed in 20 mL serum bottles and crimp sealed under atmospheric or N_2 conditions, respectively. All samples were shipped to and analyzed at the Advanced Photon Source of Argonne National Laboratory (Argonne, IL) to discern Se complexation chemistry using X-ray absorption spectroscopy at XOR/PNC Sector 20-BM. The Se K-edge (12,658 eV) XAS spectra were collected in fluorescence mode using a Canberra 13-element detector. The electron storage ring was operated at 7 GeV in top-up mode. The beamline was equipped with a Si 1 1 1 monochromator with the horizontal slit set at 6 mm and the vertical at 2.3 mm. The Se(IV) samples were placed in N_2 purged bags during data collection. Select Se(IV) samples were further analyzed under atmospheric conditions with similar results indicating beam induced oxidation was not a concern.

The collected spectra were analyzed using the Athena and Artemis software programs in the computer package IFEFFIT [32]. At least three spectra were averaged followed by subtraction of the background through the pre-edge region using the Autobk algorithm [33]. The averaged spectra were normalized to an atomic absorption of one, and the X-ray absorption fine structure (XAFS) signal was extracted from the spectra. The data were converted from energy to photoelectron momentum (k-space) and weighted by k^3. The XAFS spectra were calculated over a typical k-space range with a Hanning window and 1.0 width Gaussian wings. Fourier transforms (FT) were performed to obtain the radial distribution function (RDF) in R-space. Plotted R-space (Å) data are not phase shift corrected, the true distances are between 0.3 and 0.5 Å longer than the distances shown. The spectra were fit with the FEFF8 computer code which uses ab initio calculations to determine phase shift and amplitude functions for single and multiple atomic scattering paths. Each spectrum was fit by isolating the first shell (Se–O) to estimate the change in the threshold energy between theory and experiment (ΔE_0). The amplitude reduction factor (S_O) was constrained to be within the range of 0.80–1.0 and the Debye–Waller factor ($\Delta\sigma^2$) was allowed to float. The scattering paths used to fit the XAFS data were selected based on potential surface complexes determined by geometrically estimating potential scattering paths using theoretical crystal structures.

2.3. Experiment 2 approach

Following XAS analysis, the WTR-Se(IV), pH 7 solid phase samples were exposed, in a pH 7 buffered solution (tris(hydroxymethyl)aminomethane), to compressed air at ~14 kPa for 1, 2, 4, 7, 14, and 28 days to study potential oxidation of selenium. After selected time periods, samples were centrifuged, the supernatant discarded, and the solids were air-dried under atmospheric conditions at 25 °C. Solid phases were again analyzed using XAS.

2.4. Experiment 3 approach

In order to identify potential differences in redox state during reaction, 60 mg Se(IV) L^{-1} (0.05 M NaCl; pH 7, tris(hydroxymethyl)aminomethane) were shaken for 24 h under atmospheric conditions. The solutions were then exposed to compressed air (~14 kPa) for 28 days, centrifuged, the supernatant discarded, the solids air-dried under atmospheric conditions at 25 °C, and then analyzed using XAS.

3. Results and discussion

3.1. Experiment 1

Water treatment residuals adsorption of selenate was unaffected by pH ($p = 0.73$), although WTR adsorbed between 1400 and 2100 mg Se(VI) kg^{-1} (Fig. 2). The character of WTR-Se(VI) adsorption fell between those plotted for the combination reference clay mineral phases and the highly reactive amorphous $Al(OH)_3$. This suggested that WTR-Se(VI) adsorption was governed by the mixture of kaolinite, montmorillonite, illite–smectite, and amorphous $Al(OH)_3$ mineral phases.

The elemental composition of the WTR shows the material is approximately 7.5% Al, 1.8% Fe, and 0.1% Mn (Table 1) present as metal oxide phases or incorporated in clay minerals. Thus, the dilution of amorphous Al phases by other constituents present in WTR likely influenced the Se(VI) adsorption signature. In contrast to our findings, Bar-Yosef and Meek [18] showed that at any given concentration Se(VI) adsorption onto kaolinite decreased with increasing pH. Goldberg and Glaubig [17] found that Se(VI) adsorption on a calcareous, montmorillonitic soil did not occur across a pH range of 2–11. And in a column leaching study, Ahlrichs and Hossner [34] studied Se(VI) adsorption onto a sandy loam containing 25% clay, noting little Se(VI) retention. However, Singh et al. [35] indicated that calcium carbonate and soil clay content play an important role in Se(VI) adsorption. It appears that calcium carbonate, clays, and amorphous $Al(OH)_3$ play important roles in WTR-Se(VI) adsorption.

Water treatment residuals Se(IV) adsorption was also unaffected by pH ($p = 0.43$ on log transformed data), although WTR adsorbed a similar quantity of Se(IV) as compared to Se(VI) (1400–1950 mg Se(IV) kg^{-1}; Fig. 2). As with selenate, selenite adsorption fell between those plotted for the combination reference clay mineral phases and amorphous $Al(OH)_3$. The literature shows that Se(IV) adsorption on hydrous aluminum as well as clay minerals occurs via ligand exchange [29,36], or the replacement of oxygen ions on hydrous oxide surfaces by anions [37]. Bar-Yosef and Meek [18] noted that at any given Se(IV) concentration and pH > 7 that Se(IV) adsorption by montmorillonite exceeded that of kaolinite; at pH 5.5 the inverse relationship was obtained. Frost and Griffin [28] found that montmorillonite adsorbed more Se(IV) than kaolinite, and attributed the greater adsorption to either greater particle edge surface area or interlayer-bound hydroxy aluminum polymers. Considering these findings, our results suggest that a mixture of mineral phases, such as in WTR, should adsorb a relatively constant quantity of Se(IV) across a range of pH due to ligand exchange properties and exposed particle edge surface area of multiple mineral phases.

X-ray absorption spectroscopy of Se(VI) binding onto WTR and reference minerals as a function of pH is illustrated in Fig. 3. Across the pH range studied no shift in bonding energy existed (Fig. 3A) indicating no change in oxidation state for Se(VI) sorption on to WTR. Selenate remained as Se(VI) as would be expected for adsorption under oxic conditions. In addition, the Fourier transformed data (Fig. 3B) showed no change in the bonding environment with pH change, and the fitted data (red dotted lines) closely modeled the actual data (solid line). The bonding geometries of Se(VI) onto WTR across pH values are presented in Table 2. The Se–O shell bond distances remained at 1.64 Å while the coordination number

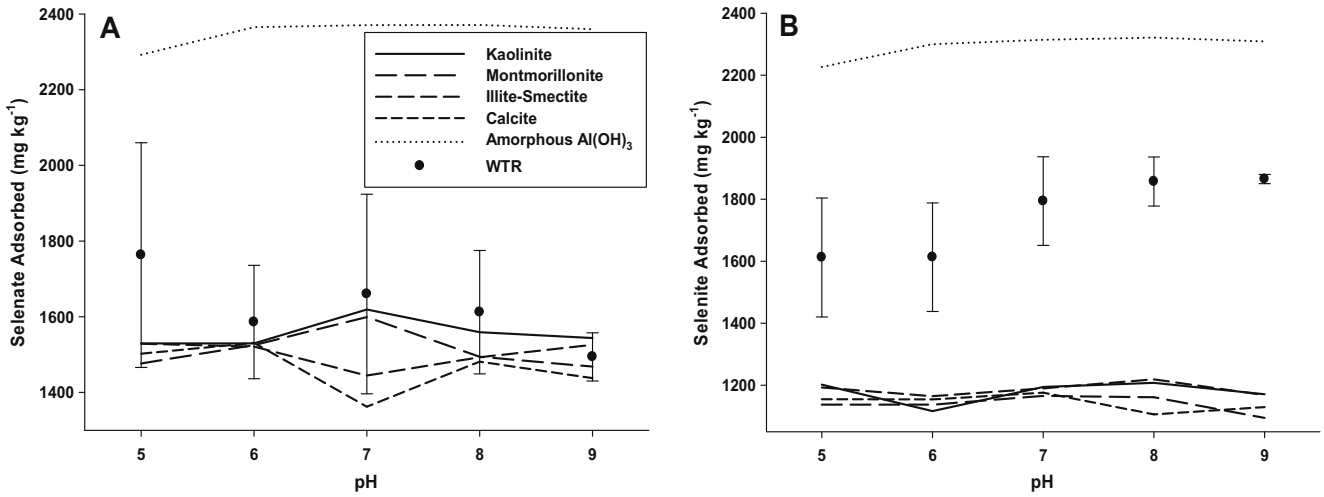

Fig. 2. Adsorption of (A) selenate and (B) selenite onto water treatment residual (WTR), kaolinite, montmorillonite, illite-smectite, calcite, and amorphous $Al(OH)_3$ as a function of pH.

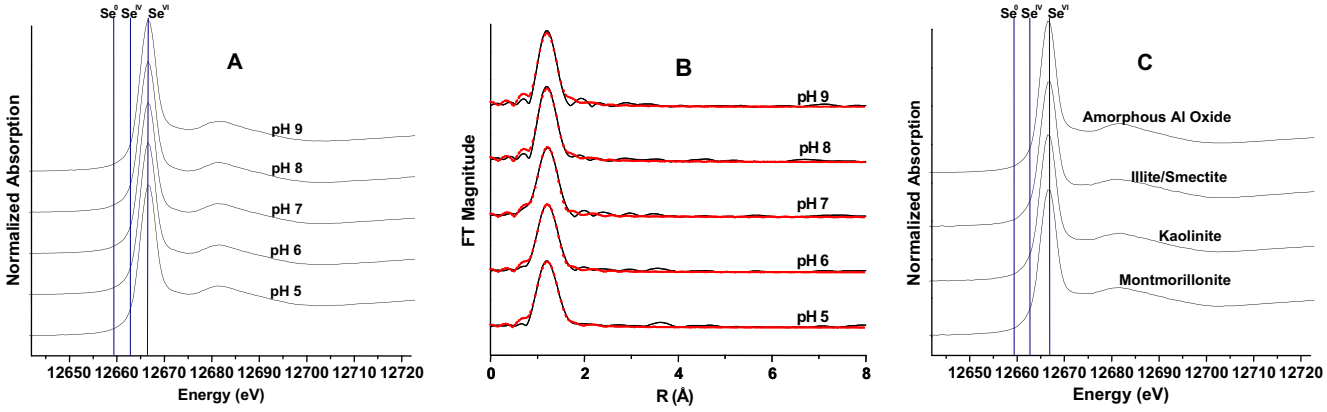

Fig. 3. Water treatment residuals normalized absorption of (A) selenate *K*-edge XAS spectra as a function of pH, (B) Fourier-transformed actual (solid line) versus fitted (dotted line) WTR-Se(VI) data, and (C) selenate *K*-edge XAS spectra as a function of mineral phase at pH 7.

remained approximately 4.00 across the pH range studied, suggestive of Se(VI) outer-sphere complexation (see illustration in Table 2). Wijnja and Schulthess [16] showed that Se(VI) adsorption on to Al oxide existed mainly as an outer-sphere complex above pH 6, while Peak [15] suggested that Se(VI) adsorption on a hydrous aluminum oxide, regardless of pH, was as an outer-sphere complex. Others have shown Se(VI) adsorption as inner-sphere complexation [12–14], although all of these studies focused on adsorption onto iron (hydr)oxide phases. The lack of inner-sphere complexation suggests that iron (hydr)oxide impurities in Al-based WTR have limited impact on selenate adsorption.

X-ray absorption spectroscopy of Se(VI) on to reference mineral phases at pH 7 is shown in Fig. 3C. Calcite was excluded due to excessive spectral noise and poor data quality in the spectra, suggesting that calcite did not play a major role in Se(VI) adsorption. Binding of Se(VI) at other pH values (pH 5, 6, 8, and 9; data not shown) were identical to binding at pH 7, with no observed shift in bonding energy or speciation. Identification of Al as a second shell neighbor of Se(VI) suggests that amorphous $Al(OH)_3$ is the main sorbent in Al-based WTR although one cannot rule out available alumina sites within clay minerals present in WTR.

X-ray absorption spectroscopy of Se(IV) binding onto WTR and reference minerals, under anoxic conditions and as a function of pH, is illustrated in Fig. 4. Examination of XAS WTR-Se(IV) adsorption data indicated a distinct shift in bond energy which favored elemental Se (Se(0)) formation across the pH range studied (Fig. 4A). In addition, the observed and fitted Fourier transformed data (Fig. 4B) supported the finding of Se(IV) reduction to Se(0). From pH 5–8, selenium was only found in the Se(0) valence state, while at pH 9 both Se(0) and Se(IV) were present. The double peak at pH 9 is present above the isoelectric point of aluminum oxide (pH 8.5), whereby increased competition for binding sites between Se(IV) and hydroxyls would occur. A reduction in adsorption sites could have ultimately increased the activation energy required to reduce Se(IV) to Se(0) and thus full reduction did not occur.

Selenium as Se(0) has been commonly considered an unavailable form of Se because of its insolubility [38]. It is not fully known why Se(IV) to Se(0) reduction in the presence of WTR occurred across the pH range examined in this study. The WTR utilized contained 6.3% organic matter (Table 1), and Singh et al. [35] found a positive correlation between soil organic carbon content and Se(IV) adsorption but did not identify selenite reduction. Absent from the literature are extensive studies of selenium reactions with Mn(II) and Mn(III) mineral oxides. The presence of 800 mg Mn kg^{-1} in the WTR may provide substantial reductants for selenite reduction, and several redox reactions for Mn mineral phases are outlined in Table 3. Unfortunately, the exact involvement of Mn in selenite reduction has yet to be demonstrated.

In an attempt to understand elevated Se levels in drainage and groundwater systems, Jayaweera and Biggar [39] examined the influence of Mn^{2+}, pH, and Eh on selenate and selenite in a continuous-flow, closed-loop soil column study. During induced soil an-

Table 2
X-ray absorption spectroscopic bonding chemistries of selenate and selenite adsorption onto Al-WTR as a function of pH under oxic and anoxic conditions, respectively, selenate and selenite adsorption onto reference mineral phases at pH 7 under oxic and anoxic conditions, respectively, anoxic and oxic selenite adsorption onto WTR followed by 4 weeks of air purging, and elemental selenium.

Sample			Se–O Shell			Se–Se Shell			Se–Al Shell		
	S_0[a]	E_0[b]	R (Å)[c]	N[d]	$\Delta\sigma^2$ (Å^2)[e]	R (Å)	N	$\Delta\sigma^2$ (Å^2)	R (Å)	N	$\Delta\sigma^2$ (Å^2)
Oxic WTR-Se(VI)											
pH 5	0.85	1.3	1.64	4.23	0.001						
pH 6	0.86	3.1	1.64	4.25	0.001						
pH 7	0.90	4.7	1.64	4.26	0.002						
pH 8	0.90	1.1	1.64	4.01	0.001						
pH 9	0.87	0.7	1.64	4.00	0.001						
Oxic reference											
Mineral phase Se(VI)											
Amorp. $Al(OH)_3$	0.85	3.8	1.64	4.00	0.001						
Illite/smectite	0.86	3.5	1.64	4.06	0.001						
Kaolinite	0.86	3.6	1.64	4.06	0.001						
Montmorillonite	0.84	3.5	1.65	4.08	0.001						
Anoxic WTR-Se(IV)											
pH 5	0.88	3.3				2.35	2.20	0.003			
pH 6	0.88	4.5				2.35	2.18	0.003			
pH 7	0.87	4.4				2.35	2.16	0.003			
pH 8	0.89	4.6				2.35	2.20	0.004			
pH 9	0.87	5.6	1.69	2.97	0.001	2.35	2.22	0.001	3.23	2.01	0.004
Anoxic reference											
Mineral phase Se(IV)											
Amorp. $Al(OH)_3$	0.90	8.8	1.70	3.18	0.001						
Illite/smectite	0.86	9.4	1.71	3.22	0.001				3.22	1.85	0.003
Kaolinite	0.86	7.8	1.70	3.08	0.002				3.16	1.97	0.004
Montmorillonite	0.89	9.6	1.71	3.23	0.001				3.23	1.91	0.006
Anoxic WTR-Se(IV) + 4 weeks air purging	0.90	4.9				2.36	2.10	0.002		2.01	0.004
Oxic WTR-Se(IV) + 4 weeks air purging	0.89	7.2	1.70	3.19	0.001				3.22	1.90	0.001
Elemental Se (monoclinic)[f]						2.35	2.20	0.004			
Elemental Se (red)[g]						2.36	2.10	0.003			

[a] Amplitude reduction factor.
[b] Energy shift.
[c] Interatomic bond distance.
[d] Coordination number.
[e] Debye–Waller factor.
[f] Ryser et al. [49].
[g] Scheinost and Charlet [43].
[h] Bond mechanism images reprinted from Peak [15] with permission from Elsevier.

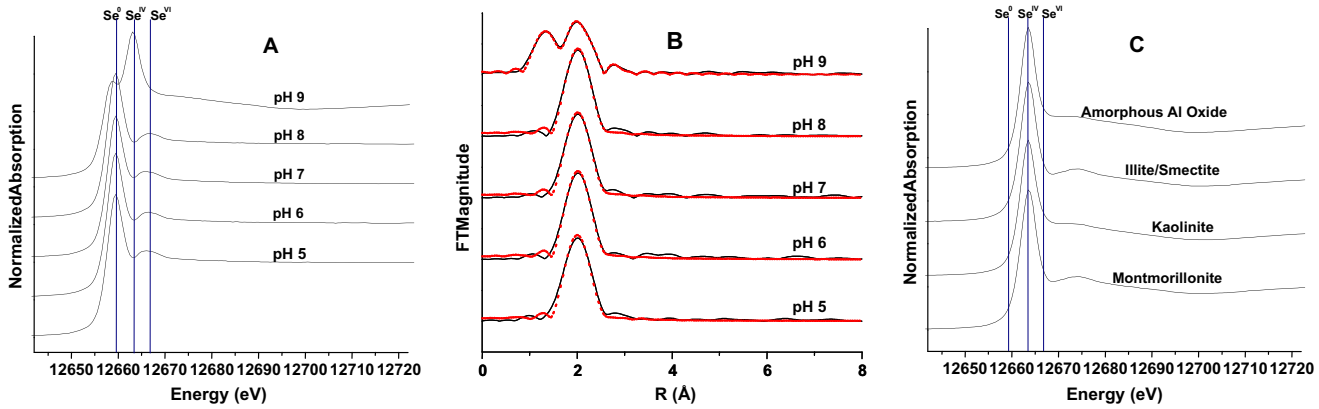

Fig. 4. Water treatment residuals normalized absorption of (A) selenite *K*-edge XAS spectra as a function of pH, (B) Fourier-transformed actual (solid line) versus fitted (dotted line) WTR-Se(IV) data, and (C) selenite *K*-edge XAS spectra as a function of mineral phase at pH 7.

Table 3
Chemical equilibrium reactions of manganese mineral species [53].

Chemical reaction	Log K°
MnO_2 (pyrolusite) + $4H^+ + 2e^- \leftrightarrow Mn^{2+} + 2H_2O$	41.89
Mn_2O_3 (bixbyite) + $6H^+ + 2e^- \leftrightarrow 2Mn^{2+} + 3H_2O$	51.46
MnOOH (manganite) + $3H^+ + e^- \leftrightarrow Mn^{2+} + 2H_2O$	25.27
Mn_3O_4 (hausmannite) + $8H^+ + 2e^- \leftrightarrow 3Mn^{2+} + 4H_2O$	63.03

oxic conditions, total soluble Se and SeO_4^{2-} decreased, while SeO_3^{2-} and other Se forms (organic Se, elemental Se, and selenide) increased initially, and then decreased. With no spectroscopic data to confirm, Jayaweera and Biggar [39] attributed decreases in SeO_3^{2-} during reduction to be partly due to the precipitation of elemental Se or $MnSeO_3$.

Clearly an unidentified phase other than the reference clay minerals, calcite, or amorphous $Al(OH)_3$ was influencing selenite reduction to Se(0) since independent selenite adsorption onto these reference phases under anoxic conditions was maintained as Se(IV) (Fig. 4C) across all pHs. Several reports on selenite reduction in the presence of zerovalent iron and ferrous iron occur in the literature [40–44] but in most of these cases the reaction requires weeks to occur relative to our 24 h reaction period. Researchers have observed rapid reduction of Se(IV) to elemental Se within 1 day by nanoparticulate mackinawite and magnetite [43] and by mixed FeII/III (hydr)oxide green rusts [44]. However, these mineral phases were not identified in the WTR material and would not expect to be present within our study reaction conditions. The presence of highly surface reactive Fe nanoparticles of other oxide forms may explain these results, although the analytical methods employed here could not identify such phases. While others have noted significant Fe concentrations in alum-derived WTR [7,45–47], identification of the Fe phases is elusive. To characterize the Fe chemistry in the Se(IV)-WTR samples, we conducted a Mössbauer spectroscopy study of the solids after the anoxic and oxic experiments and found no differences in Fe coordination and oxidation (data not shown). Based on curve fitting values and peak positions for isomer shifts and quadrupole splitting, the Fe speciation within the samples consisted of 90% ferrihydrite and 10% Fe(III) within clay structures; no identifiable peaks for ferrous iron were observed.

Since the WTR utilized in this study was taken directly from Fort Collins drinking water treatment facility, the presence of redox-active biological ligands and biofilms may also explain the reduction of selenite to elemental Se. Templeton et al. [48] conducted a selenite reduction study within *Burkholderia cepacia* biofilms formed on α-Al_2O_3 surfaces. In experiments with metabolically active *B. cepacia* biofilms on α-Al_2O_3, Se(IV) was rapidly reduced to red elemental Se and accumulated within the biofilms as discrete phases. Although Se(IV) reduction was rapid and apparent, the maximum conversion was only 50% of the initial Se(IV) concentration during the 1000 h experiment. In radiation-treated studies with non-active *B. cepacia* cells [48], selenite reduction did not occur. Despite the clear demonstration that selenite reduction was biologically mediated, the mechanism of Se(IV) reduction to Se(0) was not determined.

The bonding coordination data of Se(IV) onto WTR, under anoxic conditions and across pH values studied, are presented in Table 2. The Se–O shell bond distance for pH 9 equaled 1.69 Å and the coordination number was close to 3.00; reference mineral phases behaved similarly, suggestive of Se(IV) inner-sphere complexation (see illustration in Table 2). The Se–Al shell for WTR at pH 9 and the reference mineral phases further supports the formation of inner-sphere Se(IV) complexation. Peak [15] found similar Se–O and Se–Al shell values for Se(IV) adsorbed onto hydrous aluminum oxide at pH 8, and suggested inner-sphere complexation as the adsorption mechanism at this pH. Others have suggested Se(IV) inner-sphere complexation on goethite [12,14].

The Se–Se shell bond distances for WTR across all pH values indicated a constant bond distance of 2.35 Å and coordination number close to 2.00 (Table 2). These values were similar to those obtained from and support the formation of either monoclinic [49] or red [43] elemental Se (Table 2).

3.2. Experiments 2 and 3

In order to identify potential changes in redox state, the WTR-Se(IV) pH 7 solid phase samples from the previous anoxic experiment demonstrating Se(0) phases, and Se(IV) adsorbed onto WTR in an oxic environment with inner-sphere Se(IV) complexes, were exposed to compress air for up to 28 days. Data for day 28 are presented in Fig. 5A (all other time steps were similar), and anoxic adsorption of Se(IV) onto WTR with Se(0) reaction product is shown (lower spectra) as a reference. Interestingly, when the anoxic samples were purged with compressed air for 28 days no apparent shift in oxidation state, bond distance or coordination number occurred (Table 2). The Fourier transformed data supported the lack of Se oxidation from either the Se(0) or Se(IV) state (Fig. 5B). Previous research has shown elemental Se to be stable in reduced, aquatic systems [50], but can become unstable when a reducing environment is transited to an oxidizing environment [51]. Our results suggest that Se(0) may possibly be entrained in WTR microsites to such a degree that it was kinetically difficult

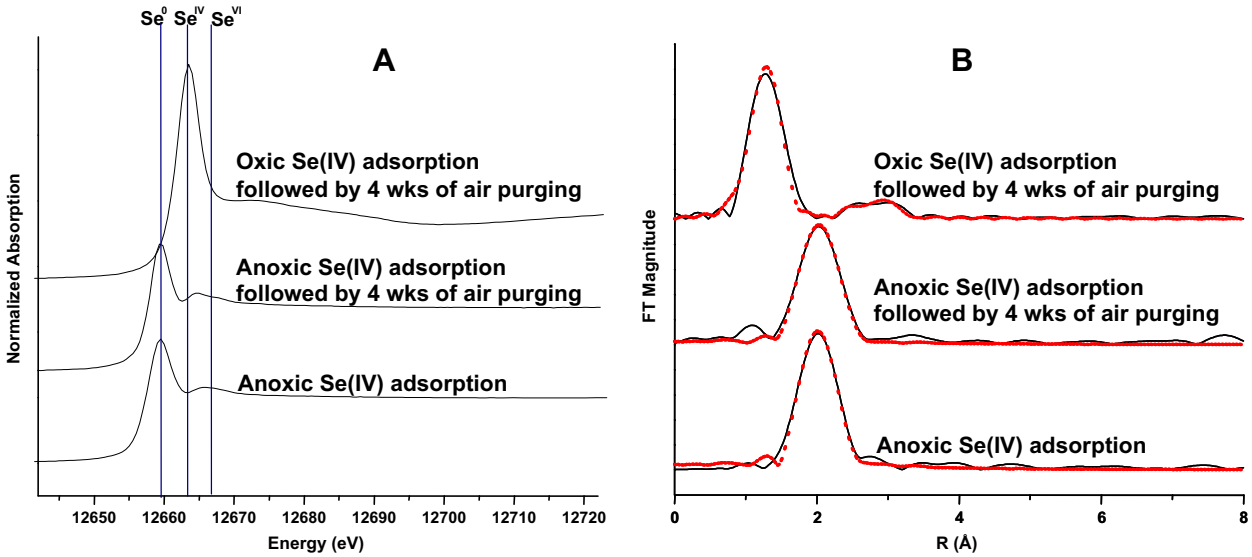

Fig. 5. Water treatment residuals normalized absorption of (A) selenite *K*-edge XAS spectra as a function of anoxic Se(IV), anoxic or oxic Se(IV) adsorption followed by 4 weeks of air purging and (B) Fourier-transformed actual (solid line) versus fitted (dotted line) data.

to oxidize. Entrainment and long-term stability has been shown to occur for phosphate trapped in WTR micropores [4].

Oxic adsorption of Se(IV) onto WTR followed by purging with compressed air for 28 days also shows no apparent change in Se speciation, Se–O and Se–Al shell bond distance and coordination number, further supporting the contention that Se(IV) microsite adsorption is aiding in retention and oxidation resistance. These findings support those of Makris et al. [52] who found that As(III) and As(V) binding were both strongly and irreversibly adsorbed by WTR with no apparent changes in oxidation state. The re-oxidation of Se(0) or oxidation of Se(IV) bound to WTR appears irreversible.

4 Conclusions

Selenium tends to accumulate in soil and water ecosystems affected by certain types of marine sediments commonly found in the western USA. Treatment strategies which target the removal of readily available selenium will reduce the bioaccumulation, deformity, and reproduction failure potential of migratory waterfowl, fish, insects, and plants in Se-sensitive areas. Our results suggest that Al-based WTR could be beneficially utilized to reduce water-borne Se concentrations regardless of redox conditions. Furthermore, Al-based WTR appear to form stable complexes with adsorbed Se(IV) and Se(0) species, lessening the likelihood of the soluble Se(VI) release into the environment following re-oxidation of reduced Se species. Thus, WTR could be employed as an amendment to sequester Se in contaminated soils and sediments, and thus improve environmental quality.

Acknowledgments

The authors acknowledge the continued research support from Fort Collins, Colorado. The PNC/XOR facilities at the Advanced Photon Source, and research at these facilities, are supported by the US Department of Energy – Basic Energy Sciences, a major facilities access grant from NSERC, the University of Washington, Simon Fraser University and the Advanced Photon Source. Use of the Advanced Photon Source is also supported by the US Department of Energy, Office of Science, Office of Basic Energy Sciences, under Contract DE-AC02-06CH11357. A portion of this research was conducted by the National Risk Management Research Laboratory of the US Environmental Protection Agency. This paper has not been subjected to the Agency's internal review. Therefore, the research results presented herein do not, necessarily, reflect the views of the Agency or its policy. Mention of a specific product or vendor does not constitute a guarantee or warranty of the product by the U.S. Dept. of Agriculture or imply its approval to the exclusion of other products that may be suitable.

References

[1] US Geological Survey, 2005, <http://menlocampus.wr.usgs.gov/50years/accomplishments/agriculture.html>.
[2] US Geological Survey, 2008, <http://co.water.usgs.gov/projects/BSD00/index.html>.
[3] US Fish and Wildlife Service, Report No. R6/714C/99, 1999, <http://www.fws.gov/mountain-prairie/contaminants/papers/kendrick.pdf>.
[4] K.C. Makris, W.G. Harris, G.A. O'Connor, T.A. Obreza, Environ. Sci. Technol. 38 (2004) 6590.
[5] J.A. Ippolito, K.A. Barbarick, D.M. Heil, J.P. Chandler, E.F. Redente, J. Environ. Qual. 32 (2003) 1857.
[6] J.M. Novak, D.M. Watts, Soil Sci. 169 (2004) 206.
[7] K.C. Makris, D. Sarkar, R. Datta, Chemosphere 64 (2006) 730.
[8] K.C. Makris, D. Sarkar, R. Datta, Environ. Pollut. 140 (2006) 9.
[9] D.L. Sparks, Environmental Soil Chemistry, second ed., Springer, San Diego, CA, 2003. pp. 138–140.
[10] N.T. Basta, J.A. Ryan, R.L. Chaney, J. Environ. Qual. 34 (2005) 49.
[11] L.S. Balistrieri, T.T. Chao, Soil Sci. Soc. Am. J. 51 (1987) 1145.
[12] K.F. Hayes, A.L. Roe, G.E. Brown Jr., K.O. Hodgson, J.O. Leckie, G.A. Parks, Science 238 (1987) 783.
[13] D. Peak, D.L. Sparks, Environ. Sci. Technol. 36 (2002) 1460.
[14] A. Manceau, L. Charlet, J. Colloid Interface Sci. 168 (1994) 87.
[15] D. Peak, J. Colloid Interface Sci. 303 (2006) 337.
[16] H. Wijnja, C.P. Schulthess, C.P. J. Colloid Interface Sci. 229 (2000) 286.
[17] S. Goldberg, R.A. Glaubig, Soil Sci. Soc. Am. J. 52 (1988) 954.
[18] B. Bar-Yosef, D. Meek, Soil Sci. 144 (1987) 11.
[19] P.N. Soltanpour, G.W. Johnson, S.M. Workman, J.B. Jones Jr., R.O. Miller, in: D.L. Sparks (Ed.), Inductively Coupled Plasma Emission Spectrometry and Inductively Coupled Plasma-mass Spectrometry, Methods of Soil Analysis, Part 3 – Chemical Methods, Soil Science Society of America, Madison, Wisconsin, USA, 1996.
[20] US EPA, SW-846, 1996, <http://www.epa.gov/epawaste/hazard/testmethods/sw846/online/index.htm>.
[21] R.L. Jones, G.B. Dreher, in: D.L. Sparks (Ed.), Silicon, Methods of Soil Analysis, Part 3 – Chemical Methods, Soil Science Society of America, Madison, Wisconsin, USA, 1996.
[22] J.M. Bremner, in: D.L. Sparks (Ed.), Nitrogen – Total, Methods of Soil Analysis, Part 3 – Chemical Methods, Soil Science Society of America, Madison, Wisconsin, USA, 1996.
[23] R.L. Mulvaney, in: D.L. Sparks (Ed.), Nitrogen – Inorganic Forms, Methods of Soil Analysis, Part 3 – Chemical Methods, Soil Science Society of America, Madison, Wisconsin, USA, 1996.

[24] G.W. Thomas, in: D.L. Sparks (Ed.), Soil pH and Soil Acidity, Methods of Soil Analysis, Part 3 – Chemical Methods, Soil Science Society of America, Madison, Wisconsin, USA, 1996.
[25] J.D. Rhoades, in: D.L. Sparks (Ed.), Salinity: Electrical Conductivity and Total Dissolved Solids, Methods of Soil Analysis, Part 3 – Chemical Methods, Soil Science Society of America, Madison, Wisconsin, USA, 1996.
[26] D.W. Nelson, L.E. Sommers, in: D.L. Sparks (Ed.), Total Carbon, Organic Carbon, and Organic Matter, Methods of Soil Analysis, Part 3 – Chemical Methods, Soil Science Society of America, Madison, Wisconsin, USA, 1996.
[27] J.D. Rhoades, in: A.L. Page, R.H. Miller, D.R. Keeney (Eds.), Cation Exchange Capacity, second ed., Methods of Soil Analysis, Part 2. Chemical and Biological Properties, American Society of Agronomy, Madison, Wisconsin, USA, 1982.
[28] R.R. Frost, R.A. Griffin, Soil Sci. Soc. Am. J. 41 (1977) 53.
[29] S.S.S. Rajan, J. Soil Sci. 30 (1979) 709.
[30] N.J. Kabengi, S.H. Daroub, R.D. Rhue, J. Colloid Interface Sci. 297 (2006) 86.
[31] SAS Institute, SAS/STAT User's Guide, Cary, North Carolina, USA, 2002.
[32] B. Ravel, M. Newville, J. Synchrotron Rad. 12 (2005) 537.
[33] M. Newville, P. Livins, Y. Yacoby, J.J. Rehr, E.A. Stern, Phys. Rev. B 47 (1993) 14126.
[34] J.S. Ahlrichs, L.R. Hossner, J. Environ. Qual. 16 (1987) 95.
[35] M. Singh, N. Singh, P.S. Relan, Soil Sci. 132 (1981) 134.
[36] R.H. Neal, G. Sposito, K.M. Holtzclaw, S.J. Traina, Soil Sci. Soc. Am. J. 51 (1987) 1161.
[37] H. Bohn, B. McNeal, G. O'Connor, Soil Chemistry, second ed., John Wiley and Sons, New York, USA, 1985.
[38] V. Astratinei, E. van Hullebusch, P. Lens, J. Environ. Qual. 35 (2006) 1873.
[39] G.R. Jayaweera, J.W. Biggar, Soil Sci. Soc. Am. J. 60 (1996) 1056.
[40] L. Charlet, A.C. Scheinost, C. Tournassat, J.M. Greneche, A. Gehin, A. Fernandez-Martinez, S. Coudert, D. Tisserand, J. Brendle, J. Geochim. Cosmochim. Acta 71 (2007) 5731.
[41] R.L.D. Loyo, S.I. Nikitenko, A.C. Scheinost, M. Simonoff, Environ. Sci. Technol. 42 (2008) 2451.
[42] A.M. Scheidegger, D. Grolimund, D. Cui, J. Devoy, K. Spahiu, P. Wersin, I. Bonhoure, M. Janousch, J Phys IV 104 (2003) 417.
[43] A.C. Scheinost, L. Charlet, L. Environ. Sci. Technol. 42 (2008) 1984.
[44] A.C. Scheinost, R. Kirsch, D. Banerjee, A. Fernandez-Martinez, H. Zaenker, H. Funke, J. Contam. Hydrol. 102 (2008) 228.
[45] S. Agyin-Birikorang, G.A. O'Connor, Sci. Total Environ. 407 (2009) 826.
[46] A.O. Babatunde, Y.Q. Zhao, Y. Yang, P. Kearney, Chem. Eng. J. 136 (2008) 108.
[47] Y. Yang, Y.Q. Zhao, P. Kearney, Chem. Eng. J. 145 (2008) 276.
[48] A.S. Templeton, T.P. Trainor, A.M. Spormann, G.E. Brown, Geochim. Cosmochim. Acta 67 (2003) 3547.
[49] A.L. Ryser, D.G. Strawn, M.A. Marcus, J.L. Johnson-Maynard, M.E. Gunter, G. Moller, Geochem. Trans. 6 (2005) 1.
[50] M.A. Elrashidi, D.C. Adriano, S.M. Workman, W.L. Lindsay, Soil Sci. 144 (1987) 141.
[51] Y. Zhang, Z.A. Zahir, W.T. Frankenberger Jr., J. Environ. Qual. 33 (2004) 559.
[52] K.C. Makris, D. Sarkar, J.G. Parsons, R. Datta, J.L. Gardea-Torresdey, J. Colloid Interface Sci. 311 (2007) 544.
[53] W.L. Lindsay, Chemical Equilibria in Soils, John Wiley and Sons, New York, USA, 1979.